International Journal of Advanced Technology in Engineering and Science
Vol. No.5, Issue No. 07, July 2017
www.ijates.com
ijates
ISSN 2348 - 7550

Structural and Dilectric Studies on Nanocrystalline Titanium Doped Manganese Zinc Ferrite Synthesized by Hydrothermal Method

R.Nagaraju[1], Ch.S.L.N.Sridhar[2], Ch.S.Lakshmi[3]

K.SivaMahalaxmi[4], V.Lakshmi, Savithri[5]

[1]Dhruva Institute of Engineering and Technologu, Toopranpet(vi),Choutuppal(M) Yadadri Bhongir (Dt), Telangana (India)

[2]Vignana Bharathi Institute of Technology, Aushapur(v), Ghatkesar(M), R.R.Dist Hyderabad, Telangana. (India)

[3]JNTUK College of Engineering, East Godavari, Kakinada, Andhra pradesh. (India)

[4]TKREC, Medbowli, Meerpet,Saroornagar, Hyderabad, Telangana (India)

ABSTRACT

$Mn_{0.5}Zn_{0.5}TixFe_{2-4x/3}O_4$ (x = 0 and 0.05) nano particles are synthesized using hydrothermal method. X-ray diffraction (XRD) technique is used to characterize the nano-particles. Particle size is calculated using Scherrer equation. Addition of Titanium increases the lattice constant. The dielectric constant and dielectric loss are found to decrease with increase in frequency. The frequency dependence of the imaginary part of the electric modulus (M″) exhibits a peak that shifts to lower frequencies with the doping content.

Keywords: Hydrothermal method, nanoparticles, scherrer equation.

I. INTRODUCTION

Nanosized manganese Zinc ferrite is found to be exhibiting interesting structural and magnetic properties. The possible applications of these ferrite nanoparticles are in magnetic storage, as precursors for ferrofluids, as contrast enhancing agents in magnetic resonance imaging (MRI), as magnetic refrigerant materials in magnetic refrigeration technology and magnetically guided drug-delivery agents **[1,2]**. Manganese Zinc ferrites belong to the class of spinel ferrites. The equilibrium distribution of cations in the bulk structure is influenced by a number of factors namely ionic radii, ionic charge, lattice energy, octahedral site preference energy and crystal field stabilization energy. For example, in the coarser regime, Zn^{2+} has a strong preference for tetrahedral sites while Ni^{2+} exhibits a strong octahedral preference in spinel ferrites. Cations like Mn^{2+} /Mn^{3+} are found to be influencing the magnetic, structural and electrical properties considerably.

II. EXPERIMENTAL

Manganese Zinc ferrites with a composition of $Mn_{0.5}Zn_{0.5}TixFe_{2-4x/3}O_4$ (x = 0 to 0.05) are prepared **[3]** byhydrothermal method. The starting materials are AR grade chemicals (Sd. Fine) of

$Mn(NO_3)_2.6H_2O$,$Zn(NO_3)_2.6H_2O$, $Fe(NO_3)_3.9H_2O$, Ti_2O_5. All the compounds are weighed with an electronic balance (Infra

Digital, INSOL) of precision 0.001gm. Then they are mixed in deionized water (AIMS Corporation, Hyderabad). Ammonia solution is slowly added till p^H is 8.0 using a p^H meter (Chemiline, India). Then the solution is Thoroughly mixed using a magnetic stirrer and transferred to an indigenously designed stainless steel autoclave of 1 litre capacity. The solution introduced into the autoclave is heated to a temperature of 200^0C for 4 hours at a pressure of 25Kg. The contents are allowed to cool, and the solution is cleaned thoroughly with deionised water and then dried in an oven at 60^0C for 24 hrs. The sample is taken out and powdered using an Agate mortar. The powder mixtures were pressed into pellets of 12mm diameter under a uni-axial pressure of 5MPa. The pellets were then sintered in a muffle furnace at a temperature of 1273k for 8hrs. The XRD pattern is studied using a X ray Diffractometer (Bruker, Germany, Model : D8) with CuK_α (λ = 1.54A).

III. X-RAY DIFFRACTION ANALYSIS

X-Ray powder diffraction technique has been used to carry out phase analysis and X-Ray densities. The XRD Patterns of $Mn_{0.5}Zn_{0.5}TixFe_{2-4x/3}O_4$ produced by hydrothermal method and sintered at 1273K are shown in Fig.1. The patterns of the samples match with the standard **[4]** JCPDS data. The patterns confirm the formation of ferrite structure. The broad XRD line indicates that the ferrite particles are of nanosize. It is also observed that a secondary peak is observed near to (311) peak. This secondary peak is due to Fe_2O_3 which is formed due to heating**[5]**.The average particle size for the composition is calculated from the XRD line width of (311) diffraction peak using Scherrer formula**[6]**.The value of the particle size and lattice parameter as deduced from the X ray data are given in Table-1.

The room temperature XRD patterns of $Mn_{0.5}Zn_{0.5}TixFe_{2-4x/3}O_4$ for x = 0 and 0.05 sintered at 1000^oC are presented in Figure-1. The peaks are labelled and identified with the corresponding planes by Miller Indices. In the wake of the reported standard XRD data, the present case of Ti doped Mn-Zn ferrite is confirmed with spinel structure. Appearance of the prominent extra peak at (104) which is nearer to the (311) peak confirms the abundance of hematite phase. In the wake of reports on Nb doped Mn-Zn ferrites, which are sintered at 900^oC, appearance of extra peak and abundance of hematite phase relevant extra peak is attributed to the low-temperature (~1000^oC) sintering conditions. The spinel structure of ferrites along with prominent (311) and (104) planes are represented in Figure-1. However, sintering carried out at higher temperature followed by mechanical milling is reported to lead to the escape of Zn^{2+} ions, and thus caused for a greater density of structural imperfections. The appearance of relatively broadened XRD peaks than that reported for bulk samples vouches for the growth of nanophased structure.

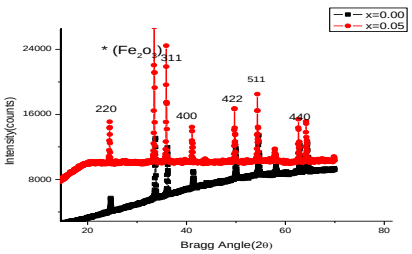

Fig.1 XRD Pattern of $Mn_{0.5}Zn_{0.5}TixFe_{2-4x/3}O_4$ for x = 0 & 0.05

Sample	Lattice constant(A^o)	Crystallite size(nm)
X=0.00	8.229	58
X=0.05	8.263	54

Table-1

The values of lattice parameter determined are presented in Table-1, and its variation with dopant (Ti) concentration is presented in Figure-2. An increase of lattice parameter is observed. When $Ti^{3+}(0.67A^0)$ replaces Fe^{3+} $(0.64A^0)$the lattice constant increases .

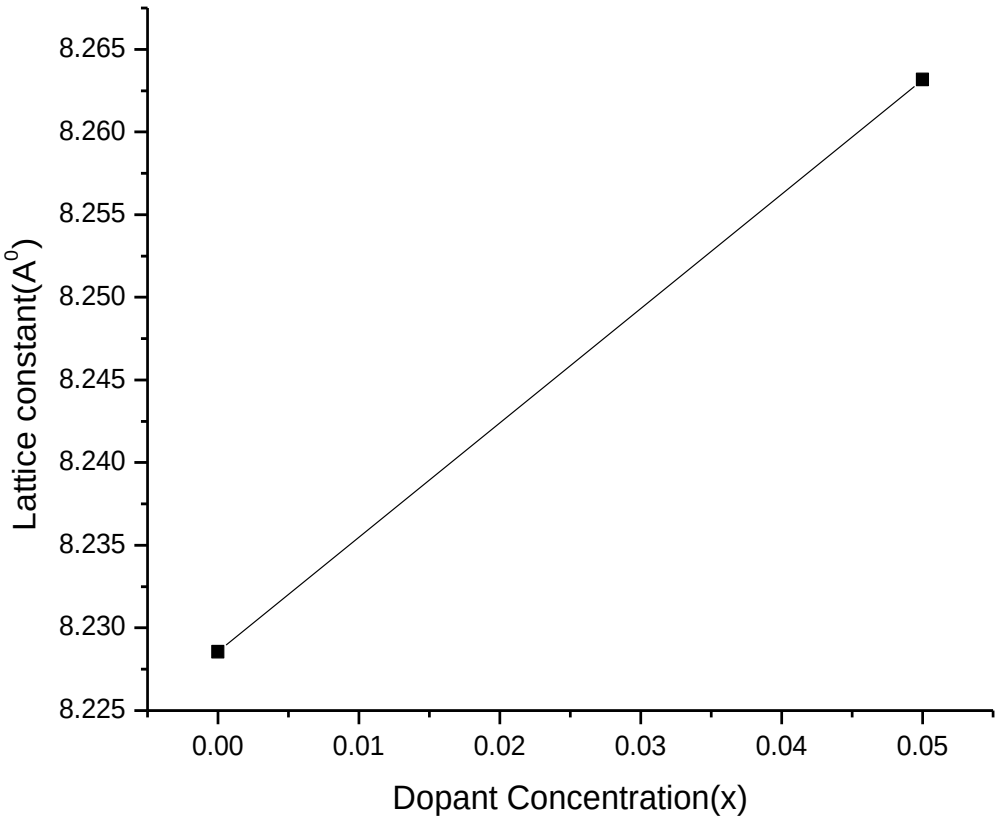

Fig-2: Variation of lattice constant With dopant concentration for Ti^{4+} doped nanocrystalline Mn-Zn ferrite

IV. VARIATION OF DIELECTRIC CONSTANT WITH FREQUENCY

The effect of frequency on the real dielectric constant (ε') can be seen from Figure-3. The value of dielectric constant decreases continuously with increasing frequency. The decrease in the values of dielectric constant as the frequency increases can be due to electron exchange interaction between $Fe^{2+}$and Fe^{3+}ions, which cannot follow the alternating electric field. The decrease of dielectric constant with increase of frequency is similar to as observed in the case of Ni-Zn ferrite. A similar behavior was also observed in various ferrite systems. The decrease of dielectric constant with increase of frequency of the applied electric field can also be explained on the

basis of Koop's theory, which assumes that the ferrites are made up of well conducting grains separated by a thin layer of poorly conducting grain boundaries[**7-10**].

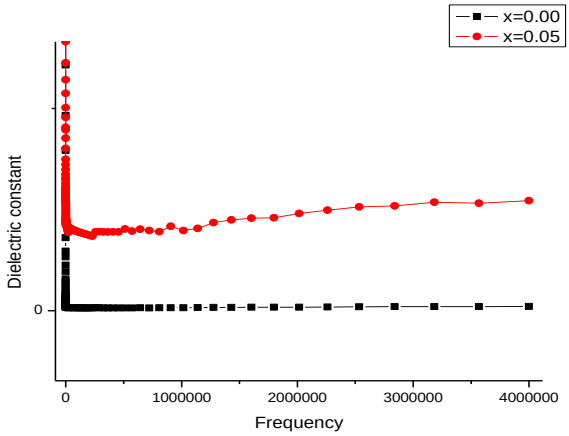

Fig-3:Variation of Dielectric constant with frequency for pure and Ti^{4+} doped nanocrystalline Mn-Zn ferrite

V. VARIATION OF DILECTRIC LOSS WITH FREQUENCY

Variation of dielectric loss factor (tan δ) with frequency (in the range of 200mHz to 4MHz) recorded at room temperature for the Ti doped nanophased Mn-Zn ferrites is illustrated in Figure-4. An overall decrease of tan δ with frequency is observed. After an initial fall, tan δ is found to attain still lower value at a particular frequency, and remains almost invariant with its further increase. The observed higher tan δ at lower frequencies and higher tanδ in high-frequency region are found to agree with predictions of Koop's model of layered dielectric structure. As pointed out by Iwauchi [**11**], there is a strong correlation between the conduction mechanism and the dielectric behavior of ferrites. The conduction mechanism in n-type ferrites is considered as due to hopping of electrons between Fe^{2+} and Fe^{3+}. The lower loss values exhibited at higher frequency reflects up on their potential applications in high-frequency microwave devices.

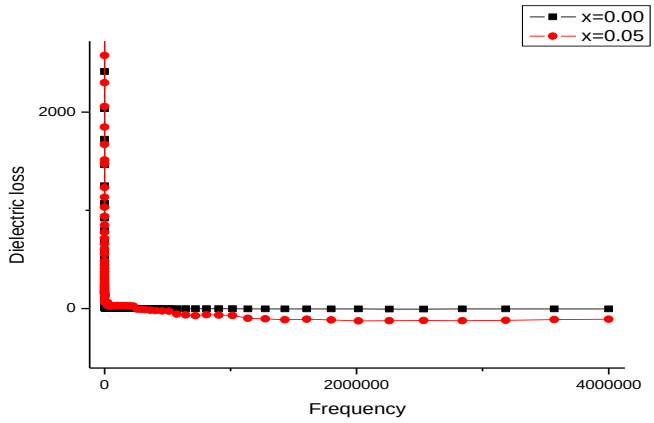

Fig-4: Variation of Dielectroc loss with frequency for pure and Ti^{4+} doped nanocrystalline Mn-Zn ferrite

VI. VARIATION OF REAL MODULUS WITH FREQUENCY

The variation of real part of electric modulus (M') as a function of frequency is shown in Figure-5. The value of M' is very low in the low frequency region. As frequency increases the value of M' increases and reaches a maximum constant value of $M\infty = 1/\varepsilon_\infty$ at higher frequencies. These observations may possibly be related to a lack of restoring force governing the mobility of charge carriers under the action of an induced electric field. These features indicate that the electrode polarization makes a negligible contribution in the material[**12**].

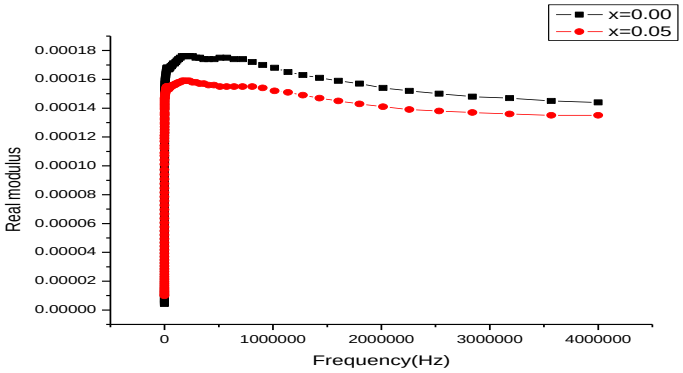

Fig-5: Variation of Real Modulus with frequency for pure and Ti^{4+} doped nanocrystalline Mn-Zn ferrite

VII. VARIATION OF IMAGINARY MODULUS WITH FREQUENCY

The frequency dependence of the imaginary part of the electric modulus (M'') exhibits a maximum in Figure-6. It may be noted that the position of the peak shifts to lower frequencies as the doping content is increased. This pattern provides wider information relating charge transport processes such as mechanism of electrical transport, conductivity relaxation, and ion dynamics as a function of frequency. The frequency region below the peak maximum determines the range in which charge carriers are mobile over long distances. At the frequency above peak maximum (high-frequency), the carriers are confined to potential wells, being mobile over short distances.

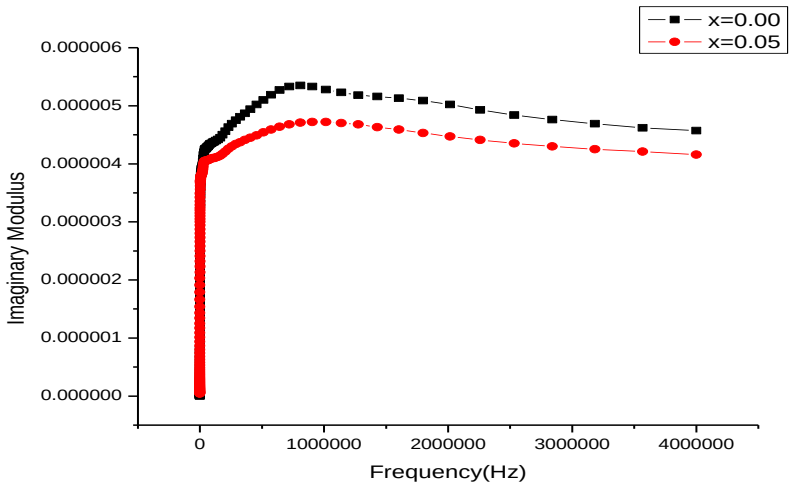

Fig-6: Variation of Imaginary Modulus with frequency for pure and Ti^{4+} doped nanocrystalline Mn-Zn ferrite

VIII. CONCLUSIONS

1. Hydrothermal method has been successfully used to synthesize nanocrystalline Manganes Zinc ferrite.
2. The XRD Studies confirm the formation of Ferrite structure.
3. The crystallite size calculated from Scherrer equation is 58nm for pure ferrite and 52nm for Ti doped ferrite.
4. The dielectric constant and dielectric losses of the doped Manganese-Zinc ferrites are decreased by increasing the frequency of the applied AC field, representing the typical behavior of the ferrites, caused by the lagging of the hopping electrons behind the changing frequency of the applied AC field.
5. Improved tenability of dielectric constant and conductivity by adopting low temperature sintering conditions.

REFERENCES

[1] S. Sun, C.B. Murray, D. Weller, L. Folks, A. Moser, Science 287 (2000) 1989.

[2] Q.A. Pankhurst, J. Connolly, S.K. Jones, J. Dobson, J. Phys. D: Appl. Phys. 36 (2003) R167.

[3] Sarika D. Shinde , G. E. Patil, D. D. Kajale, D. V. Ahire1, V. B. Gaikwad and G. H. Jain , International journal on smart sensing and intelligent systems, Vol. 5, No. 1,March 2012.

[4] P.Bayliss, D.C.Erd, M.E.More, A.Sabina and D.K. Smith, Mineral Powder Diffraction, JCPDS, USA, 1986.

[5] Rozman M. and Drofenic M., J. Am. Ceram.Soc. 78 (1995) 2449 – 55.

[6] B.D.Cullity "Elements of X-Ray diffraction" Addison-Wesley publishing Co.inc,(1978).

[7] D. Ravinder *Ph. D. Thesis,* Osmania University, 1988.

[8] M. A. El Hiti *J. Magn. Magn. Mater.* 164 (1996) 187.

[9] E. Melagiriyappa, H. S. Jayanna and B. K. Chougule *Mater. Chem. Phys.* 112 (2008) 68.

[10] Q. Chen, P. Du, W. Huang, L. Jin, W. Weng and G. Han *Appl. Phys. Lett.* 90 (2007) 132907.

[11] K. Iwauchi *Japan. J. Appl. Phys.*, 10 (1971) 1520.

[12] Chowdari B.V.R., Gopalakrishnan R. (1987): AC conductivity analysis of glassy silver iodomolybdate system.*Solid State Ionics*, *23*(3), 225-233. doi: 10.1016/0167-2738(87)90055-5.